EAST EUROPEAN JOURNAL OF PHYSICS. **3.** 319-324 (2025)
DOI:10.26565/2312-4334-2025-3-30 ISSN 2312-4334

SURFACE MORPHOLOGY AND ROUGHNESS OF SULFUR-DOPED ZnO THIN FILMS: ANALYSIS BASED ON ATOMIC FORCE MICROSCOPY

Akramjon Y. Boboev[a], Nuritdin Y. Yunusaliyev[a], Khushroy A. Makhmudov[b], Fayzuloh A. Abdulkhaev[a], Gaybullo G. Tojiboyev[a], Mohlaroyim O. G'ofurjonova[a]
[a]*Andijan state university named after Z.M. Babur, Andijan, Uzbekistan*
[b]*Kokand University Andijan branch, Andijan, Uzbekistan*
**Corresponding Author E-mail: aboboevscp@gmail.com*
Received March 30, 2025; revised July 9, 2025; accepted July 20, 2025

The surface morphology of undoped ZnO as well as 3 at. % sulfur-doped ZnO (ZnO:S) thin films were examined utilizing atomic force microscopy (AFM). Surface characteristics evaluations and comparisons were made based on 2D and 3D AFM images, line profile analyses, and roughness parameters; R_a, R_q, R_z, R_t R_{sk}, and R_{ku}. The undoped ZnO medium showed a smooth surface, with moderate height fluctuations and a comparatively narrow Gaussian-like height. On the other hand, ZnO:S film showed much higher surface roughness and topographical alternation with larger and more symmetrical height histograms. Both the R_q/R_a ratios for both started at around the theoretical Gaussian value (~1.25) with the skewness and kurtosis parameters showing distinctly different degrees of surface symmetry and texture. Sulfur incorporation was shown to change the grain morphology, to introduce peak-to-valley contrast and to increase the overall surface area. The morphological improvements further show that ZnO:S thin films could be more adequate for applications where high surface activity is essential, provided by gas sensing and catalysis. This study presents a quantitative and qualitative evaluation of the influence of sulfur doping on the surface morphology of ZnO at the nanoscale level.
Keywords*: Morphology; Histogram; Atomic force microscopy; Roughness; Doping; Sulfur*
PACS: 78.30.Am

INTRODUCTION

Thin films of zinc oxide (ZnO) have been extensively studied for their diverse applications in optoelectronics, gas sensors, catalysts, and so on, because of their excellent optical, electrical, and catalytic properties [1–3]. The surfaces have a key influence on their performance as they affect surface area, grain boundaries, and active sites for surface reactions [4,5]. Atomic force microscopy (AFM) is a proven dominant tool for the morphological characterization of surfaces that offers the images of surface textures in nanoscale and also allows a quantitative determination of surface roughness parameters [6,7]. Dopants like Al, S, and N into ZnO thin films were also studied which had considerable implications on the structural, electrical, and optical properties [8–11]. Especially, the sulfur doping can increase the surface area and modify the grain boundaries of ZnO, which can improve the gas-sensing property and catalytic activity [12,13]. Zainabidinov et al. investigated the influence of gamma radiation on the electrophysical characteristics of sulfur-doped ZnO films, noting that irradiation caused structural changes [14]. Likewise, structural and morphological properties of Al-doped ZnO films have been studied and it has been exhibited that the doping in ZnO causes a change in the grain size and its distribution [15]. Additional studies performed in our laboratory focused on elucidating structural properties by means of X-ray diffraction and electron microscopy, demonstrating significant morphological changes produced by sulfur doping in ZnO films synthesized by ultrasonic spray pyrolysis [16]. Moreover, Zainabidinov et al. have tuned an ultrasonic spray pyrolysis system for the deposition of metal oxide films with improved uniformity and structure [17]. Other investigations have elucidated defect formation in metal-insulator-semiconductor (MIS) structures based on silicon doped with rare-earth elements, potentially up to moderate concentrations, opening the pathway for understanding how doping modifies morphological and electrophysical properties. However, notwithstanding a number of studies, a broad statistical description of the morphological differences amongst undoped and sulfur-doped ZnO thin films at the nanoscale is undocumented. More advanced characterizations employing amplitude parameters like average roughness (Ra), root mean square roughness (Rq), skewness (Rsk), kurtosis (Rku), and peak-to-valley height (Rt) are required to provide a complete understanding of surface structure–function relationships. This paper studies the influence of sulfur doping on those surfaces using atomic force microscopy (AFM), in an effort to fill this gap in the literature. In summary, by carefully analyzing statistical parameters of surface roughness and relating them with probable functional dynamism, this work sheds valuable light in pathways for future exploration and evolution of ZnO materials for emerging technological domains.

MATERIALS AND METHODS

As the base material, monocrystalline n-type silicon (Si) wafers with a (100) crystallographic orientation were selected due to their high purity and compatibility with thin film deposition. The wafers were cut into rectangular pieces measuring

Cite as: A.Y. Boboev, N.Y. Yunusaliyev, Kh.A. Makhmudov, F.A. Abdulkhaev, G.G. Tojiboyev, M.O. G'ofurjonova, East Eur. J. Phys. 3, 319 (2025), https://doi.org/10.26565/2312-4334-2025-3-30

approximately 2 mm × 2 mm × 5 µm for experimental use. To improve surface smoothness and cleanliness, a multi-step treatment was performed. Initially, the substrate surface was mechanically polished using abrasive papers with 3 µm and 0.5 µm grit sizes, sequentially. This process significantly reduced the surface roughness. After polishing, substrates were rinsed with deionized (DI) water. To remove organic, inorganic, and metallic contaminants, the wafers were subjected to standard RCA cleaning. In the RCA-1 step, substrates were immersed in an NH_4OH:H_2O_2:H_2O (1:1:5) solution at ~75 °C for 15 minutes, followed by thorough DI water rinsing. The RCA-2 step involved immersion in HCl:H_2O_2:H_2O (1:1:6) at the same temperature and duration to eliminate metal ions. Finally, the native SiO_2 oxide layer on the wafer surface was etched in a 5% HF solution for 1 minute, and the cleaned substrate was immediately rinsed and dried to prevent reoxidation. Zinc acetate dihydrate ($Zn(CH_3COO)_2 \cdot 2H_2O$, >99%, Sigma-Aldrich) was used as the zinc source. For the undoped ZnO films, precursor solutions of 0.5 M and 1 M concentrations were prepared by dissolving the appropriate amount of zinc acetate in deionized water and stirring until complete dissolution. Specifically, 10.97 g of $Zn(CH_3COO)_2 \cdot 2H_2O$ was dissolved in 100 mL of DI water to obtain a 0.5 M solution. For sulfur doping, thiourea (CH_4N_2S, >99%, Sigma-Aldrich) was used as the sulfur source. A doping concentration of 3 atomic percent (at%) was targeted by calculating the required thiourea amount relative to the total anion content in the solution. Based on a 1:1 molar ratio of Zn to O in ZnO, 0.0015 mol of sulfur atoms were needed for 3 at% doping, which corresponds to approximately 0.114 g of thiourea for 0.05 mol of Zn precursor. Thiourea was added to the prepared zinc acetate solution and stirred thoroughly to ensure homogeneity. Thin films of ZnO and sulfur-doped ZnO (ZnO:S) were deposited on the prepared Si substrates using the ultrasonic spray pyrolysis technique [17]. The deposition was performed under controlled conditions, with optimized parameters for spray rate, substrate temperature, and carrier gas flow (not detailed here). Immediately after the HF etching step, substrates were transferred for coating to minimize surface reoxidation and maintain chemical reactivity.

Atomic Force Microscopy (AFM) was used to analyze the surface morphology and topography of the deposited films. 2D and 3D AFM images were acquired over a 500 × 500 nm scan area. Roughness parameters such as R_a, R_q, R_t, and R_z were calculated, along with statistical descriptors like skewness (R_{sk}) and kurtosis (R_{ku}). Additionally, line profiles and histogram analyses were used to assess height distribution symmetry and uniformity across the samples.

RESULTS AND DISCUSSION

2D AFM Images of Surface Morphology for Undoped ZnO and 3 at. Topography images of ZnO:S thin films with a concentration of 3 at.% sulfur, obtained on an area of 500 nm × 500 nm scale (Figure 3 but with two samples showed in comparison), show fundamental differences in surface structure. The surface of undoped ZnO film is smoother and more uniform, with larger grains available, lacking noticeable grain boundaries. This means that the crystallites merged into a surface with a much lower height difference during the film growth. This sample shows low surface roughness, suggesting that the height across the scanned point is not fluctuating heavily. In sharp contrast to this, the ZnO:S sample shows a highly textured surface and well separated fine nanograins that are very densely packed. You have multi-grain with smaller size, which can lead to a surface structure that is more heterogeneous and complex. The improved nanostructuring is probably a result of the effects of sulfur doping on the nucleation kinetics during the formation of the film, leading to a higher amount of nucleation centers. The distinct morphologies suggest that the sulfur doping has a strong influence on the surface growth of the ZnO films, which results in denser coalescence of the grains, sharper grain boundaries, and higher surface area. In-contrast to pure ZnO, where the surface activity is depicted by a relatively low rate of charge reaction, several such modifications have been reported introducing higher surface-related functionalities, making ZnO:S more favorable in the context of high surface activity applications.

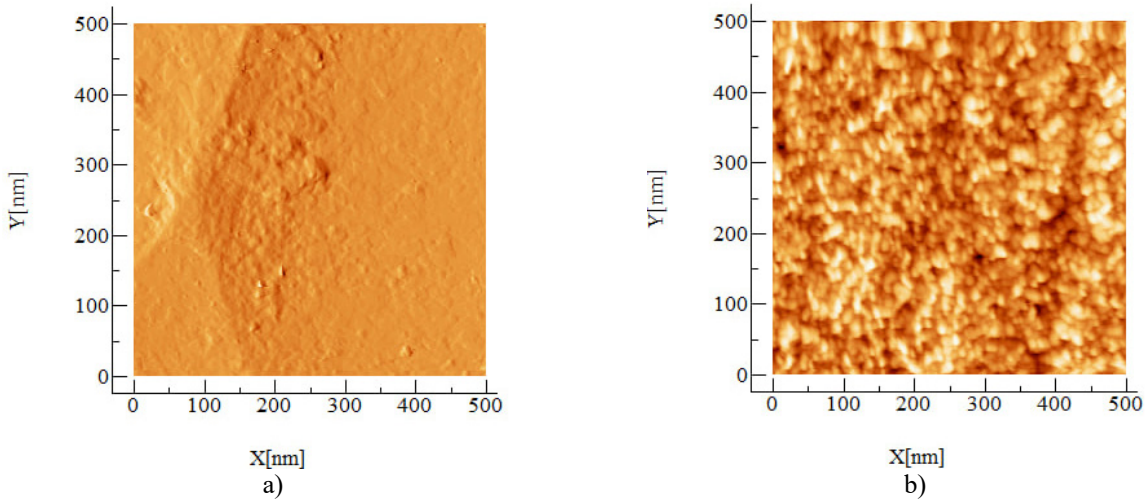

Figure 3. 2D AFM surface morphology images of thin films scanned over a 500 nm × 500 nm area. a) ZnO; b) S doped ZnO

Figure 4 shows 3D AFM topography images will reveal even more details of the surface features for each sample. The 3D perspectives give a better sense of peak-to-valley height differences as well as surface texture roughness.

A typical moderately textured surface can be seen in the undoped ZnO film featuring a clear grain elevation although the features seem less defined and broader. There are fewer grain peaks which are also more widely separated from each other, which is consistent with the earlier identification of a relatively smooth, low-roughness morphology. Contrasting with it, the rough surface of ZnO:S film, with an arrangement of sharp peaks and valleys uniformly in the scanned area, is very noticeable. The nanograins are smaller, denser, and well separated which assists in better vertical variation in the Z-axis. Higher density of nucleation sites during film growth arising from incorporation of sulfur leads to again higher surface roughness as indicated here. ZnO:S provides a highly complex surface with an increased surface area which should have functional benefits. The enhanced light scattering, increased surface reactivity and better sensitivity of the rougher and rougher morphology in optoelectronic and sensing applications [18].

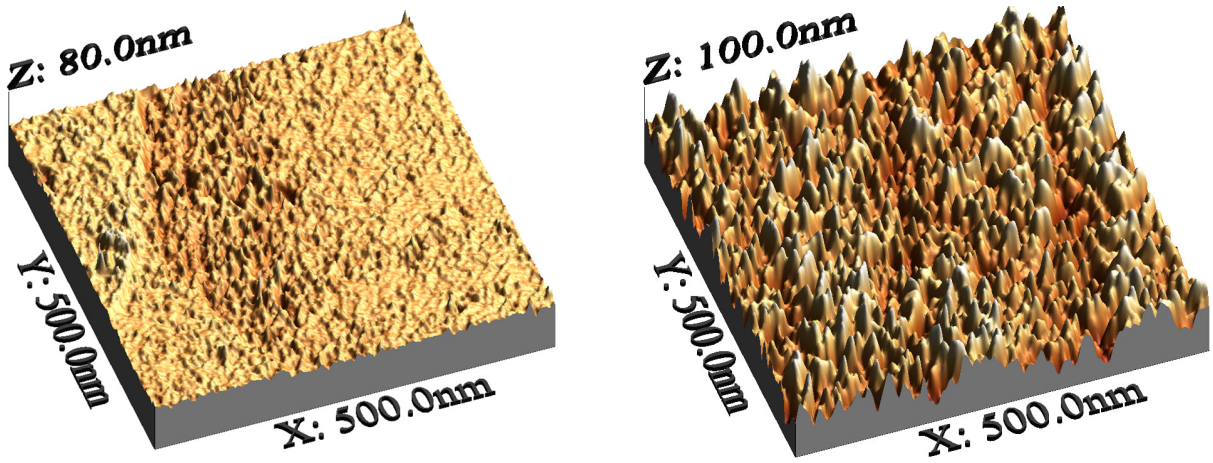

a) **b)**

Figure 4. 3D AFM topography of ZnO and ZnO:S thin films over a 500 nm × 500 nm area, revealing differences in vertical surface features and roughness. a) ZnO; b) S doped ZnO

Before delving into the quantitative surface profile results, it is essential to understand the key amplitude parameters used in AFM surface topography analysis. These parameters provide critical insights into the statistical features of a surface, including average height levels, asymmetry, and extreme height variations. One of the most widely used metrics is the average roughness (R_a), which quantifies the mean deviation from the central line and serves as a general indicator of surface uniformity and quality. The root mean square roughness (R_q) provides a more sensitive measure by considering the squared deviations from the mean line and is particularly important in high-precision optical surface evaluation. The maximum peak-to-valley height (R_t) defines the total relief of the surface and indicates the full vertical range of topographic variation. In contrast, the ten-point height roughness (R_z) calculates the average difference between the five highest peaks and the five deepest xvalleys, making it suitable for assessing local irregularities. To evaluate the shape and symmetry of the height distribution, skewness (R_{sk}) and kurtosis (R_{ku}) are employed. A negative R_{sk} implies a surface dominated by valleys, while a positive Rsk suggests dominant peaks. The kurtosis R_{ku} indicates whether the surface texture is spiky ($R_{ku} > 3$), flat and bumpy ($R_{ku} < 3$), or normally distributed ($R_{ku} \approx 3$). Together, these parameters form a comprehensive statistical framework to evaluate and compare surface characteristics across thin film samples.

Table 1 demonstrates that the changes in average roughness (R_a) and ten-point mean height (R_z) correspond closely with the variations observed in RMS roughness (R_q) across all examined samples. The maximum peak-to-valley height (R_t) remains a key indicator of surface topography, as it effectively captures the overall vertical relief of the surface. Furthermore, it is evident from Table 1 that higher R_t values are typically associated with increased R_z values, indicating a strong relationship between R_z and the extreme height differences in the surface profile. The mathematical expression for R_z is given below:

$$R_z = \frac{1}{n}\left(\sum_{i=1}^{n} P_i - \sum_{i=1}^{n} V_i\right) \tag{1}$$

where n is the number of sampling points along the assessment length, which is 5 in this study, P_i is the height of the i^{th} peak and V_i is the depth of the i^{th} valley with respect to the line profile. In addition, R_q values for all the samples are higher than Ra values, which can be mathematically explained according to the following equation:

$$R_z = \frac{1}{L}\int_0^L |y(x)|\, dx \tag{2}$$

$$R_q = \sqrt{\frac{1}{L}\int_0^L |(y(x))^2|\, dx} \tag{3}$$

where L is the length of the profile on the x-axis used for measurement and y(x) is the variation of the height from the profile line for each data point.

For surfaces exhibiting Gaussian height distributions, theoretical models suggest that the ratio of root mean square roughness (R_q) to average roughness (R_a) approaches a value of 1.25. According to Ward [19], many engineering surfaces can be reasonably approximated by a Gaussian distribution, with typical R_q/R_a ratios extending up to around 1.31. In our study, as shown in Table 1, the calculated R_q/R_a values for all three materials—Si, ZnO, and ZnO:S—are in close agreement with the theoretical prediction, indicating that the surface profiles follow an approximately Gaussian distribution at the nanometer scale. his finding validates the use of standard statistical surface roughness descriptors in characterizing the samples. Additionally, the skewness values provide insight into the asymmetry of the height distribution. Negative skewness reflects a surface dominated by valleys, while positive skewness indicates a prevalence of elevated features. In our results, skewness variations between the samples suggest different degrees of surface uniformity and grain structure. Furthermore, the kurtosis (R_{ku}) parameter reveals the nature of surface texture—whether it is spiky or bumpy. A value of R_{ku} less than 3 corresponds to a bumpy surface with fewer extreme features, while R_{ku} greater than 3 indicates a spikier texture with pronounced peaks and valleys. For instance, the ZnO:S sample demonstrated a R_{ku} value close to 3, suggesting a balanced distribution of surface features, whereas undoped ZnO exhibited a higher R_{ku}, indicative of a more irregular and spiky morphology. These trends are consistent with the R_t and R_z values, as kurtosis is strongly influenced by the amplitude of surface extremes.

$$R_{ku} = \frac{1}{NR_q^4}\left(\sum_{i=1}^{N} Y_i^4\right) \tag{4}$$

Where R_{ku} is the RMS roughness parameter and Y is the height of the profile at point number i

Table 1. Roughness parameters.

Materials	R_a nm	R_q nm	R_t nm	R_z nm	R_q/R_a	R_{sk}	R_{ku}
ZnO	2.5976	3.7144	79.9983	43.6536	1.4299	-0.6842	8.2098
S doped ZnO	8.4809	10.8674	100.0075	49.9415	1.2814	-0.005	3.3892

Such observation is confirmed by the computed roughness parameters presented in Table 1. The S-doped ZnO sample has much larger average roughness (R_a) and root mean square roughness (R_q) values than undoped ZnO as the incorporation of sulfur clearly increases the complexity of the surface (no flake-like structure). For both samples, the R_q/R_a ratio approaches the theoretical limit of the nominal Gaussian distribution (~1.25), as evident by the ratios of 1.4299 for ZnO and 1.2814 for ZnO:S, confirming that both surfaces yield approximately the same Gaussian distribution. Values for skewness (R_{sk}) also indicate asymmetry of surface features. The ZnO film shows a negative skewness value of -0.6842, indicating a surface with deep valleys predominating. On the other hand, the near zero skewness (-0.005) of the ZnO:S film reflects an approximately even topographical structure without a strong dominance of peaks or valleys. Another parameter is kurtosis (R_{ku}), which enhances the interpretation. The high value of R_{ku} = 8.21 of ZnO sample indicates that this surface is also spiky and irregular with very extreme value of height variation. In contrast, the ZnO:S display a kurtosis value of 3.39, which is significantly closer to the Gaussian ideal ($R_{ku} \approx 3$) indicating a distribution that has more uniformity, morphology-wise, which is bumpier. This, in addition to the maximum peak-to-valley height (R_t) and ten-point roughness (R_z), confirms the topographically balanced and statistically homogeneous surface resulting from sulfur doped Si core. Such surface features can improve selected functions, like an increased surface area for sensing or catalytic interactions.

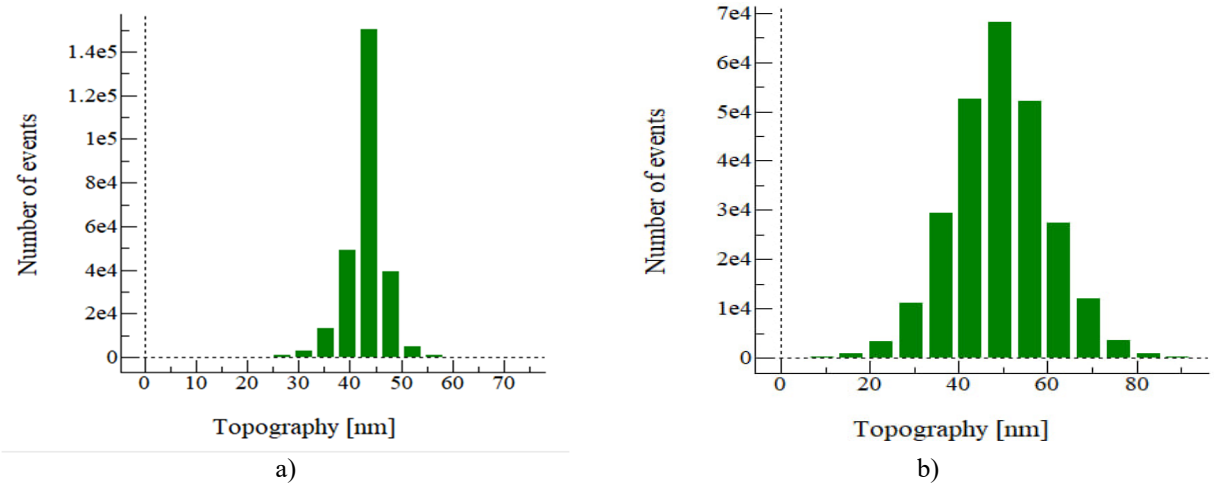

Figure 5. Height distribution histograms. a) ZnO; b) S doped ZnO

In an effort to gain insight into the statistical behavior of the surface morphology, we analyzed the height distribution histograms and numerical roughness parameters of both the ZnO and S-doped ZnO thin films. The histogram (Figure 5) provides a visual clear depiction of the distribution of topographical features on the scanned surface.

The crystalline particle size distribution of the ZnO gives a very narrow and sharply peaked distribution centered around 55 nm which means a relatively less rough surface with a relatively more even distribution. In comparison, the histogram of the S-doped ZnO sample displays a wider, more symmetrical distribution centered around 50 nm, implying a surface with more topographical deviation and a greater diversity of nanostructures.

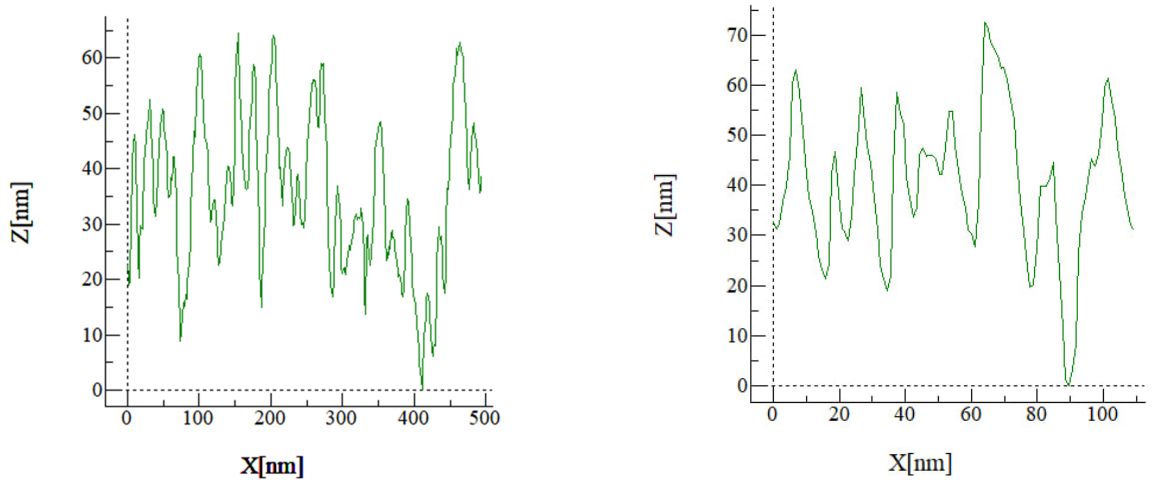

Figure 6. Line profile analysis showing the surface height fluctuations. a) ZnO; b) S doped ZnO

The line profile analysis for the as-deposited ZnO and S-doped ZnO thin films are depicted in Figure 6 and is useful to evaluate the vertical surface height variations within a span of 100 nm. Moderate variations in height (4 nm to 10 nm) can be seen in the ZnO film (Figure 6a), indicating a relatively smooth and uniform surface with minor topographical irregularities. This was also observed in the histogram data, as we saw a narrow and symmetric height distribution centered at 50 nm, indicating an overall less complex surface morphology. Compared to the ZnO:S film (Fig. 6b), which exhibits obviously bigger vertical fluctuations with a thickness of 5 nm to 25 nm. It implies that the water bodies could adjust to an increase in surface roughness indicating a surface with a more intricate structure featuring peaks and valleys. These results help confirm the above observations, as also evidenced by the broader and more symmetrical histogram distribution of the S-doped sample, indicating the more complex feature of the surface brought by the nitrogen doping. The increased height fluctuations of the ZnO:S film are due to sulfur incorporation and modification of the grain structure, increasing the surface roughness. In summary, analysis of the line profiles supports the histogram results and confirms the higher surface complexity of the ZnO:S thin films. The enhanced roughness values indicate that sulfide doping increases the surface area, potentially useful for applications such as gas sensors or catalysis, where high surface reactivity is favorable.

CONCLUSIONS

In this study, the surface morphology of ZnO and S-doped ZnO thin films was analyzed using atomic force microscopy (AFM) and key statistical parameters such as average roughness (R_a), root mean square roughness (R_q), peak-to-valley height (R_t), and skewness (R_{sk}). The results indicate a clear contrast in the surface characteristics between undoped ZnO and S-doped ZnO films. ZnO films exhibited a relatively smooth and uniform surface with moderate height variations ranging from 4 nm to 10 nm. These results were supported by the narrow height distribution observed in the histograms, indicating a less complex surface morphology. On the other hand, the ZnO:S films demonstrated significantly higher surface roughness, with height variations reaching up to 25 nm. The broader and more symmetrical histogram distribution confirmed the increased surface complexity brought about by sulfur doping. The analysis of the line profiles and histograms indicated that sulfur incorporation into ZnO modifies the grain structure and increases surface roughness. The R_q/R_a ratio for both films approached the theoretical Gaussian value, confirming the Gaussian distribution of surface height. The skewness and kurtosis values further highlighted the differences in surface symmetry and texture. ZnO:S films exhibited more pronounced surface features with balanced peaks and valleys, while ZnO films showed a dominance of valleys.

These results suggest that sulfur doping enhances the surface area and complexity of ZnO films, making them potentially more suitable for applications that require high surface reactivity, such as in gas sensing or catalytic processes. The findings provide a comprehensive understanding of how surface morphology can be tailored through doping and offer valuable insights for optimizing functional thin film applications.

Conflict of Interests

The authors declare that they have no conflict of interests

Funding

The present research work was financed under the project FZ-292154210 granted by the Ministry of Innovative Development of the Republic of Uzbekistan

ORCID
A.Y. Boboev, https://orcid.org/0000-0002-3963-708X; **N.Y. Yunusaliyev**, https://orcid.org/0000-0003-3766-5420
Kh.A. Makhmudov, https://orcid.org/0009-0004-8845-8741; **F.A. Abdulkhaev**, https://orcid.org/0009-0004-3933-5171
G.G. Tojiboyev, https://orcid.org/0009-0000-5022-8108; **M.O. G'ufurjonova**, https://orcid.org/0009-0009-8830-9371

REFERENCES

[1] Z. Zhang, Y. Chen, H. Liu, *et al*., Sens. Actuators B Chem. **344**, 130218 (2021). https://doi.org/10.1016/j.snb.2021.130218
[2] R. Kumar, and O. Al-Dossary, J. Mater. Sci. Mater. Electron. **33**, 927 (2022). https://doi.org/10.1007/s10854-021-07491-8
[3] X. Chen, H. Yu, J. Sun, *et al*., Catal. Sci. Technol. **13**, 734 (2023). https://doi.org/10.1039/D2CY01807D
[4] M. Hasanpour, S. Hatamie, and H. Zare, Appl. Surf. Sci. Adv. **2**, 100025 (2020). https://doi.org/10.1016/j.apsadv.2020.100025
[5] D. Sharma, K.M. Batoo, and S. Singh, Mater. Sci. Semicond. Process. **151**, 106986 (2022). https://doi.org/10.1016/j.mssp.2022.106986
[6] P. Eaton, and P. West, *Atomic Force Microscopy*, (Oxford University Press, 2020).
[7] S. Moreno-Flores, Prog. Mater. Sci. **120**, 100816 (2021). https://doi.org/10.1016/j.pmatsci.2021.100816
[8] A. Wei, Y. Huang, Y. Wang, *et al*., Thin Solid Films **713**, 138341 (2020). https://doi.org/10.1016/j.tsf.2020.138341
[9] H. Hamrouni, H. Saidi, and A. Bouzidi, Mater. Today Commun. **26**, 102019 (2021). https://doi.org/10.1016/j.mtcomm.2020.102019
[10] R. Mohan, and V. Krishnakumar, J. Mater. Sci. Mater. Electron. **32**, 14053 (2021). https://doi.org/10.1007/s10854-021-06044-9
[11] C. Jayachandraiah, V. Sreenivasulu, and M. Sundararajan, Optik **219**, 165051 (2020). https://doi.org/10.1016/j.ijleo.2020.165051
[12] H. J. Kim, S. Y. Kim, and J. H. Lee, Sens. Actuators B Chem. **307**, 127675 (2020). https://doi.org/10.1016/j.snb.2019.127675
[13] Y. Liu, X. Wang, and M. Zhang, J. Alloys Compd. **867**, 158986 (2021). https://doi.org/10.1016/j.jallcom.2021.158986
[14] S. Zainabidinov, A.Y. Boboev, and N.Y. Yunusaliyev, East Eur. J. Phys. (2), 321 (2024). https://doi.org/10.26565/2312-4334-2024-2-37
[15] S. Zainabidinov, Sh.Kh. Yulchiev, A.Y. Boboev, *et al*., East Eur. J. Phys. (3), 282 (2024). https://doi.org/10.26565/2312-4334-2024-3-28
[16] S. Z. Zaynabidinov, ShU Yuldashev, A. Y. Boboev, and N. Y. Yunusaliyev, Her. Bauman Moscow State Tech. Univ. Ser. Nat. Sci. **1**, 78 (2024).
[17] S.Z. Zainabidinov, A.Y. Boboev, N.Y. Yunusaliyev, and J.N. Usmonov, East Eur. J. Phys. (3), 293 (2024). https://doi.org/10.26565/2312-4334-2024-3-30
[18] M.K. Karimov, U.O. Kutliev, S.B. Bobojonova, and K.U. Otabaeva. Physics and Chemistry of Solid State, **22**(4), 742 (2021). https://doi.org/10.15330/pcss.22.4.742-745
[19] M. Nosonovsky, and B. Bhushan, J. Appl. Phys. **105**, 104303 (2009). https://doi.org/10.1063/1.3130404

МОРФОЛОГІЯ ПОВЕРХНІ ТА ШОРСТКІСТЬ ТОНКИХ ПЛІВОК ZnO, ЛЕГОВАНИХ СІРКОЮ: АНАЛІЗ НА ОСНОВІ АТОМНО-СИЛОВОЇ МІКРОСКОПІЇ

Акрамджон Й. Бобоєв[a], Нурітдін Й. Юнусалієв[a], Хушрой А. Махмудов[b], Файзулох А. Абдулхаєв[a], Гайбулло Г. Тоджибоєв[a], Мохлароїм О. Гофурджонова[a]
[a]Андижанський державний університет імені З.М. Бабура, Андижан, Узбекистан
[b]Андижанська філія Кокандського університету, Андижан, Узбекистан

Морфологію поверхні нелегованого ZnO, а також тонких плівок ZnO (ZnO:S), легованого 3 ат.% сіркою, досліджували за допомогою атомно-силової мікроскопії (АСМ). Оцінку та порівняння характеристик поверхні проводили на основі 2D та 3D АСМ-зображень, аналізу профілю ліній та параметрів шорсткості; Ra, Rq, Rz, Rt Rsk та Rku. Нелеговане середовище ZnO мало гладку поверхню з помірними коливаннями висоти та порівняно вузькою гаусівською висотою. З іншого боку, плівка ZnO:S показала значно вищу шорсткість поверхні та топографічне чергування з більшими та симетричнішими гістограмами висоти. Обидва співвідношення Rq/Ra починалися приблизно з теоретичного гаусівського значення (~1,25), причому параметри асиметрії та ексцесу демонстрували чітко різні ступені симетрії поверхні та текстури. Було показано, що введення сірки змінює морфологію зерен, вводить контраст між піками та западинами та збільшує загальну площу поверхні. Морфологічні покращення також показують, що тонкі плівки ZnO:S можуть бути більш адекватними для застосувань, де важлива висока поверхнева активність, що забезпечується газовим зондуванням та каталізом. Це дослідження дає кількісну та якісну оцінку впливу легування сіркою на морфологію поверхні ZnO на нанорівні.

Ключові слова: *морфологія; гістограма; атомно-силова мікроскопія; шорсткість; легування; сірка*